Stress Corrosion Cracking of Al-5%Mg (5083) Alloy

Shuhei OSAKI*

(Received July 23, 1974)

Abstract

Stress corrosion cracking of Al–5%Mg (5083) alloy was studied in a NaCl+HCl aqueous solution. Intergranular corrosion and stress corrosion cracking are closely correlated with the grain boundary β precipitate and both occured extremely when this precipitate was quite continuous. The crack propagation is discontinuous and the contribution of mechanical rupture is found in the process of cracking. Mechanical rupture, however, plays only a supplemental part. The crack propagation rate can be expressed as an exponential function of the intergranular corrosion rate. The stress corrosion cracking may be essentially a manifestation of intergranular corrosion facilitated by a mechano-chemical effect.

Introduction

Al–Mg alloys are generally characterized by good mechanical properties, excellent resistance to corrosion and ease of welding. Although these alloys have widely been employed for structural applications, alloys of higher magnesium content are not recommended for service by reason of causing stress corrosion cracking. Alloys containing more magnesium in solid solution than equilibrum concentration tend to precipitate β compound at grain boundaries when being naturally aged for many years or heated at slightly elevated temperatures[1,2]. This precipitate is strongly anodic to the Al–Mg solid solution matrix[3] and corrodes selectively at a high rate[4,5,6]. Thus it has been considered that a continuous grain boundary precipitate produces a susceptibility to intergranular corrosion and stress-corrosion cracking. Although 5083 alloy, containing less magnesium than 5% and additional elements of manganese and cromium, has been fabricated taking account of resistivity to stress corrosion cracking, it is not completely immune under conditions of unsuitable heat treatment or service temperature. The evaluation of susceptibility to stress-corrosion cracking and the understanding of cracking mechanism are not quite sufficient even at present.

In this study stress-corrosion cracking was tested for a hot-rolled thick plate Al–5%Mg (5083) alloy in a NaCl+HCl aqueous solution. Effects of temperature and heating time were investigated in relation to intergranular corrosion, and cracking mechanism was discussed through the observation of crack propagation and electron fractography.

* Department of Mechanical Engineering, Technical Junior College of Yamaguchi University

Experimental Procedures

Specimen

The material employed is a hot-rolled plate with 100 mm thickness, offered by SKY Aluminum Co. Ltd. The chemical compositions are shown in **Table 1**. An optical microstructure of as-received material is shown in **Fig. 1**, which represents remarkable structural anisotropy due to rolling. The differences of mechanical properties for specimens machined out in longitudinal and short transverse directions of the plate are shown in **Table 2**. Specimens for stress-corrosion tests are in the shape of bend beam, as shown in **Fig. 2** and are all taken in the short transverse direction with the major notch parallel to both the original rolling plane and direction.

Table 1 Chemical composition of 5083 aluminum alloy (wt%).

Cu	Si	Fe	Mn	Mg	Zn	Cr	Ti	Al
0.04	0.14	0.18	0.97	4.72	0.02	0.12	0.01	RE

Table 2 Mechanical properties of 5083–O aluminum alloy.

direction	0.2% yield strength Kg/mm²	tensile strength Kg/mm²	elongation %	V-notch Charpy impact value Kg-m/cm²	bending strength Kg/mm²
short transverse	13.8	29.8	12.4	0.95	42.5
longitudinal	13.7	33.5	27.6	2.47	—

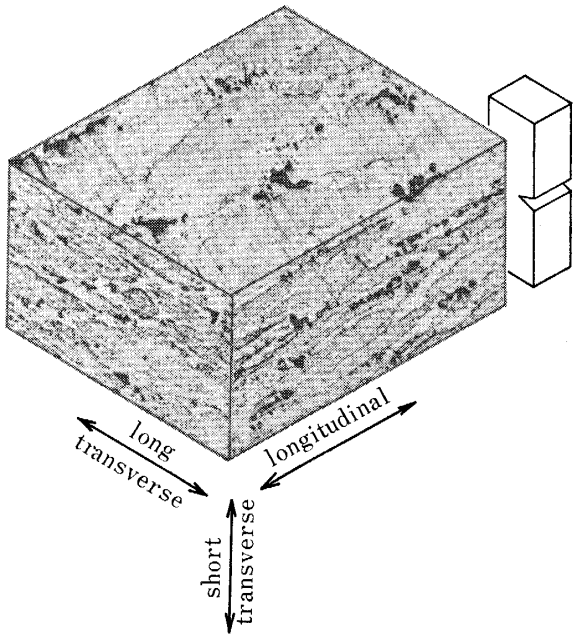

Fig. 1 Optical microstructure of 5033–O aluminum alloy.

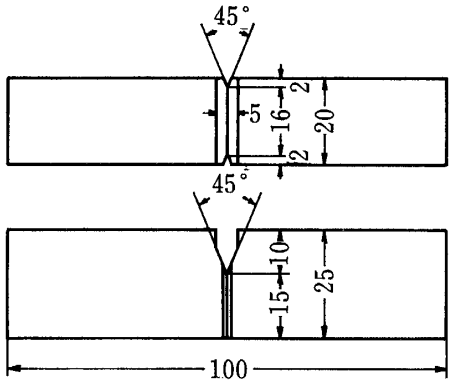

Fig. 2 Dimensions of stress corrosion test specimen.

Heat Treatment

After solid-solution treated for 24 hrs. at 450°C and water quenched, specimens were heated for several hours to 100 days at various temperatures until 300°C.

Stress-Corrosion Tests

Stress-corrosion tests were conducted by using the constant load cantilever beam technique. A schematic diagram of experimental setup is presented in **Fig. 3**. The environmental container, attached to the specimen, consisted of a flexible rubber cup of approximately 150 cm^3 volume. Only the notched area of a specimen was exposed to environment, the other surface insulated. The environment used was constant immersion in 3% NaCl + 0.5% HCl aqueous solution, renewed once a week. Crack propagation was measured as a function of beam deflection using a linear transducer mounted vertically.

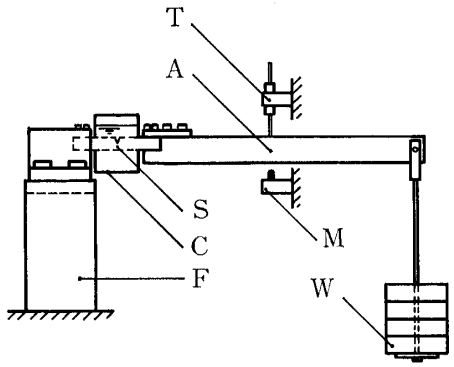

Fig. 3 Schematic diagram of apparatus for stress corrosion test
(S: specimen, C: corrosion cell,
A: loading arm, W: dead weight,
T: transducer, M: microswitch,
F: frame)

Intergranular Corrosion Tests

Tensile tests on pre-corroded specimen were made to determine loss of mechanical property because of intergranular attack. Tensile specimens with $8\phi \times 30$ mm gauge length were mechanically polished and then electro-polished in a $HClO_4 + C_2H_5OH$ solution, followed by washing and drying. Then these were subjected to a constant immersion test in 3% NaCl + 1% HCl solution. The tensile test was conducted using a Instron type machine, with a tensile rate of 1 mm/min.

Small cubic specimens were also immersed and corrosion rate was determined from

weight loss. The depth of intergranular attack was measured by metallographic sectioning of the specimen.

Fractographic Observation

A stress-corrosion cracked specimen was picked out of the corrosion cell immediately after final rupture and prepared for fractographic observation. Fracture surface morphology was examined by scanning electron microscopy.

Results and Discussions

Effects of the Heat Treatment on Intergranular Corrosion

For specimens heated for 1 week at various temperatures between 20° and 300°C, the effects of pre-corrosion on tensile strength and elongation are shown in **Fig. 4**. The tensile property itself depends hardly upon heating temperature, while for pre-corroded specimens, the remarkable effect of temperature is apparent, undergoing significant loss of strength and reduction of elongation at temperatures in the range 100°~200°C. The loss of strength results from reduction of the sectional area, not due to general dissolution but intergranular corrosion. Thus, a reduction ratio of tensile strength, $k=(\sigma_z-\sigma'_z)/\sigma_z$, can be taken as an index of intergranular corrosion susceptibility, where σ_z and σ'_z are tensile strengths of specimens without and with pre-corrosion respectively. The effect of heating temperature on k and weight loss, Δw, is shown in **Fig. 5**. On raising the temperature above 100°C, Δw increases, a maximum occurring near at 180°C, and then decreases to only a small value at higher temperature than 200°C.

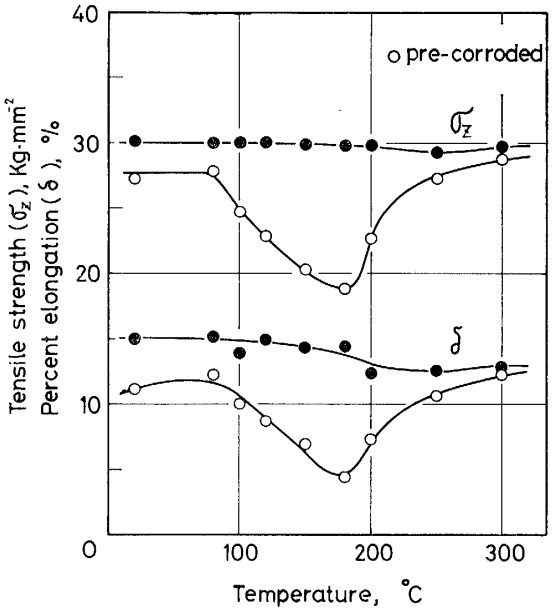

Fig. 4 Tensile strength and percent elongation of 5083 alloy heated 1 week at various temperatures, with and without pre-corrosion for 72 hrs. in 3%NaCl+1% HCl solution.

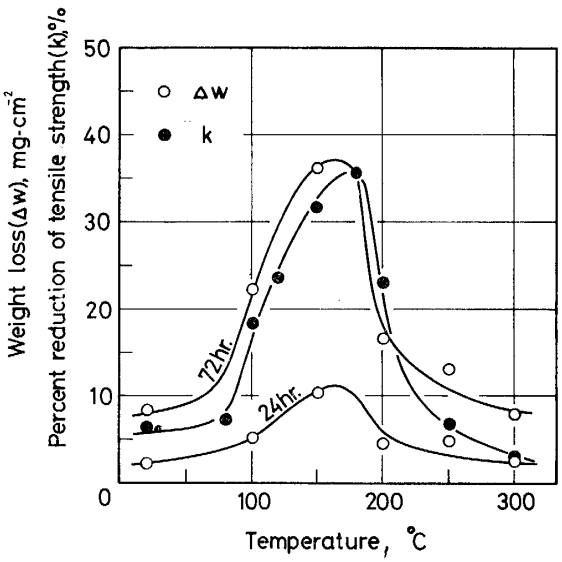

Fig. 5 Weight loss and percent reduction of tensile strength of 5083 alloy haeted 1 week at various temperatures, when immersed in 3% NaCl+1%HCl solution.

In this graph, the change of k is similar to that of Δw and therefore it is known that most of weight loss may be owing to attack at grain boundaries. Examples of intergranular attack for specimens immersed for 24 hrs. are shown in **Fig. 6**. The specimen heated at 180°C shows extensive intergranular corrosion (Fig. 6–c). Microstructures of these specimens on a parallel plane to the original rolling plane are shown in **Fig. 7**. As-quenched material represents supersaturated solid solution and by heating the excess magnesium tends to precipitate preferentially at grain boundaries as an Al–Mg compound, designated β (Mg_2Al_3) or β' phase[1,2]. As shown in Fig. 7–a, no indication of grain boundary precipitate is found in the specimen aged for 1 week at room temperature, although some insoluble β are retained in the grain matrix. With increasing temperature, however, grain boundaries begin to be outlined by precipitate and a nearly continuous grain boundary network of β phase is formed at 180°C. At higher temperatures than 200°C the amount of precipitate decreases again.

From these results it is confirmed that there is a close correlation between the amount of grain boundary precipitate and intergranular corrosion, maximum suscep-

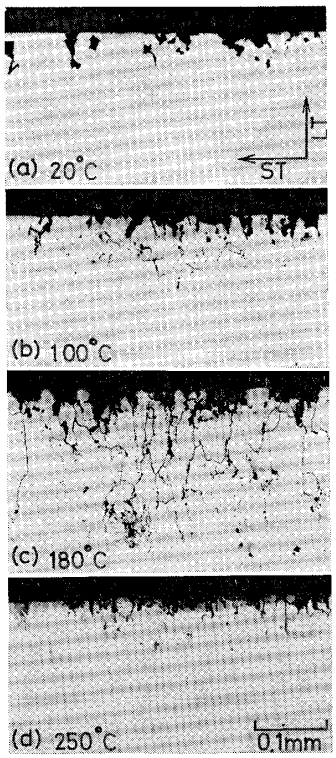

Fig. 6 Examples of intergranular cororsion of 5083 alloy heated 1 week at various temperatures, immersed 24 hrs. in 3% NaCl +1% HCl solution.

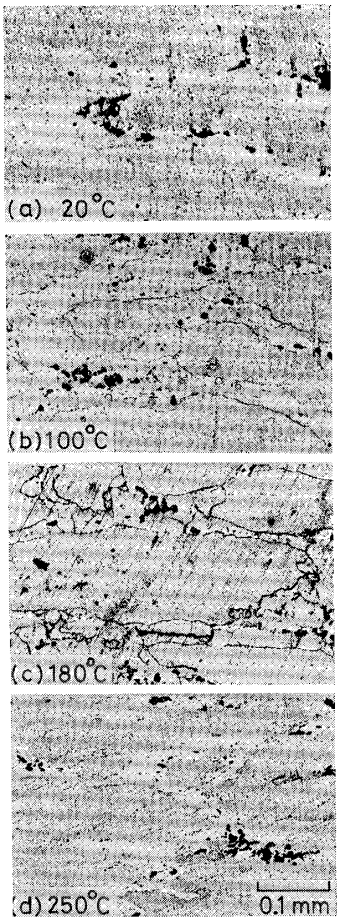

Fig. 7 Optical microstructures of 5083 alloy, heated for 1 week at various temperatures. Keller's etch.

tibility occurring at about 180°C when this precipitate is almost quite continuous. On the other hand, when it is present little or discontinuous, intergranular corrosion does not grow, but pits and small trenches generate (Fig. 6–a and 6–d).

The effect of heating times on intergranular corrosion was also investigated. The relation between weight loss (Δw) and heating time (t_h) at a constant temperature of 100°C was obtained as shown in **Fig. 8**. The variation of intergranular corrosion depth (D) is shown in the same Figure too. Both Δw and D increase with heating time and these time-dependences appear to be almost equivalent to each other. **Fig. 9** shows the relation between corrosion rate ($\Delta w/\Delta t$) and log t_h, obtained according to Fig. 8. Then corrosion rate is given by

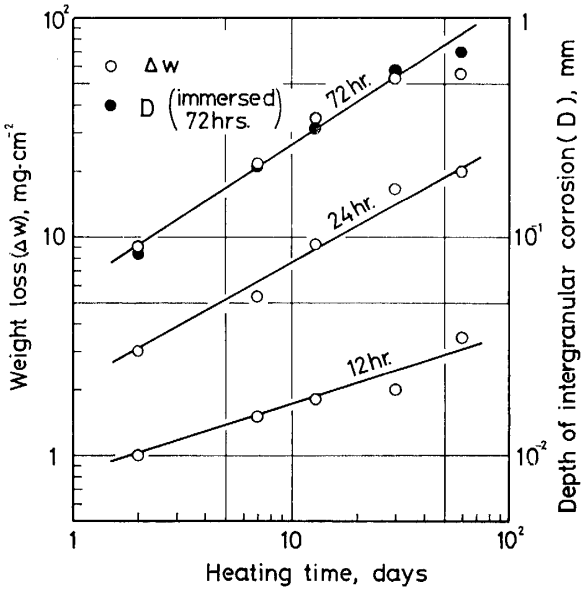

Fig. 8 Weight loss and depth of intergranular corrosion of 5083 alloy heated various times at 100°C immersed in 3% NaCl+1% HCl solution

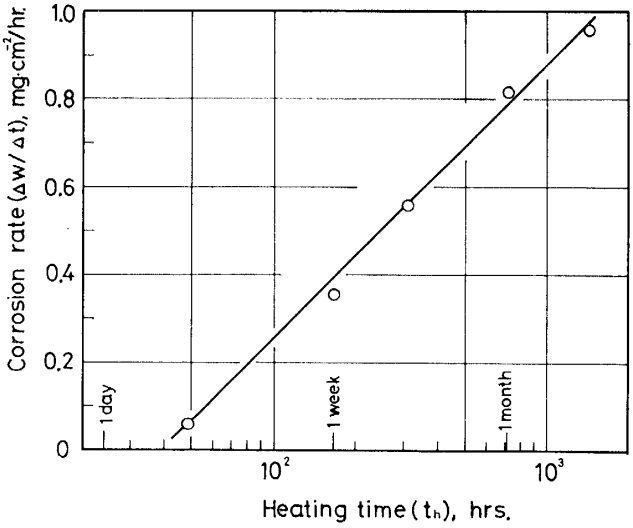

Fig. 9 Relation between corrosion rate and heating time for 5083 alloy heated at 100°C immersed in 3% NaCl+1% HCl solution.

$$\Delta w/\Delta t = k_1 + k_2 \log t_h \tag{1}$$

where k_1 and k_2 are constants. With long time heating even at lower temperature (100°C), grain boundaries are outlined enough with β precipitate. This precipitate is strongly anodic to the Al–Mg solid solution matrix in the presence of many electrolytes[3,7]. Therefore a continuous grain boundary precipitate provides an effective path for selective corrosion.

Stress-Corrosion Tests

Stress-corrosion tests were carried out on specimens heated for one week at temperatures up to 300°C. Applied stress is constant, $\sigma = 23$ kg/mm^2, with respect to a nominal bending stress at the notch root, because of no changes of yield strength and tensile strength with heating temperature as shown previously. The effect of heating temperature on stress-corrosion life is shown in **Fig. 10**. In materials heated at 80°~200°C, stress-corrosion cracking occurs, especially with a maximum susceptibility at 180°C. The cracking is always intergranular. However on raising the temperature still further, the life increases longer than 1000 hours and any crack growth is not found by microscopic observations. It is noticed that such a variation of stress-corrosion cracking susceptibility is in a good correlation with that of intergranular corrosion and also the presence of the continuous grain boundary precipitate may be directly relatable to stress-corrosion cracking too.

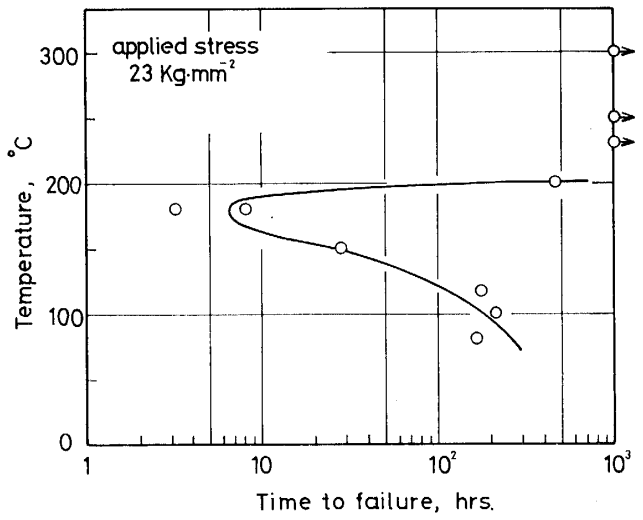

Fig. 10 Time to failure of 5083 alloy heated 1 week at various temperatures.

In order to examine the effect of heating time, the same stress-corrosion tests were conducted on specimens heated for various periods at 100°C. The obtained relation between time to failure (t_f) and heating time (t_h) is shown in **Fig. 11**. On a logarithmic plot, the curve is a straight line whose equation is given by

$$\log t_f = k_3 + k_4 \log t_h \tag{2}$$

where k_3 and k_4 are constants. Because the right term is proportional to intergranular

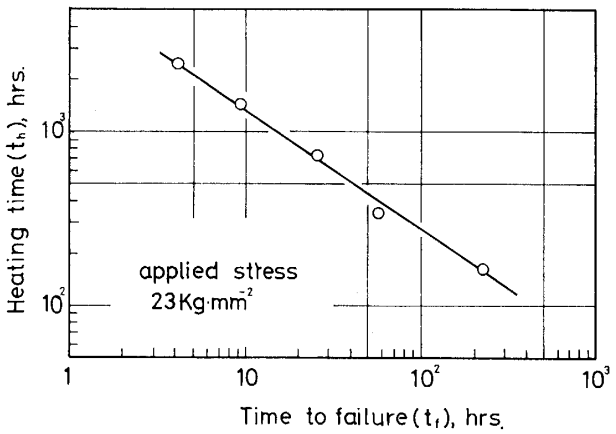

Fig. 11 Relation between time to failure and heating time for 5083 alloy heated at 100°C.

corrosion rate as given by eq. (1), equation (2) can be written as follows,

$$1/t_f = c_1 \exp(c_2 \Delta w/\Delta t) \tag{3}$$

where c_1 and c_2 are constants. It is namely indicated that the stress-corrosion life is directly dependent of intergranular corrosion rate when stress and the other mechanical factors are constant. Therefore stress-corrosion cracking of this alloy may be principally controlled by electrochemical dissolution of pre-existent paths associated with grain boundary β precipitate.

The relation between applied stress and time to failure for specimens heated for 30 days at 100°C is shown in **Fig. 12**. The curve plotted on a log scale consistes of two straight line branches, with a folding point being approximately 21 kg/mm^2 and below this point the life increasing. McEvily and Bond[8] in studies on stress-corrosion cracking of α-brass found that crack propagation rates were proportional to K_I^2, where K_I is the stress-intensity factor, and indeed the time to failure depended inversely on the square of the applied stress. From the upper side branch of the curve in Fig. 12, the

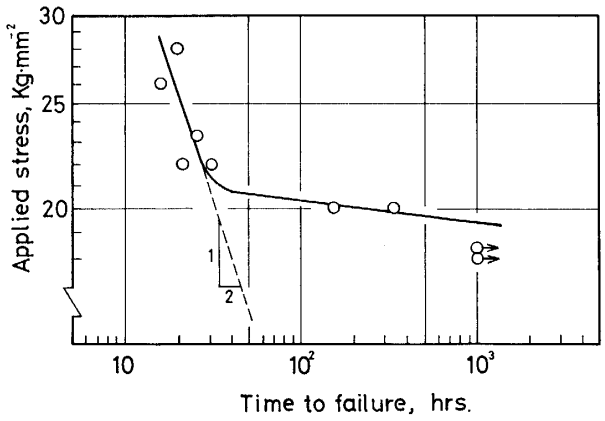

Fig. 12 Relation between time to failure and applied stress for 5083 alloy heated 30 days at 100°C.

similar relation is found to be held good. Namely provided the crack propagation is governed by electrochemical intergranular attack, it is suggested that the corrosion rate would be enhanced by mechano-chemical reactions in proportion to the square of the applied stress.

Fractography

Fig. 13 is an example of fracture surface of a specimen heated for 60 days at 100°C, showing typical intergranular stress-corrosion fracture originating from the notch root (Fig. 13–a) and mechanical final fracture (Fig. 13–b). The latter exhibits dimple and tear ridge pattern characteristic transgranular ductile fracture. The stress-corrosion fracture extends for considerable distances on grain boundaries parallel to the original rolling plane, representing only smooth and featureless aspects, nor any evidence of river pattern or striation[9]. However with extension of the crack, regions probably due to mechanical rupture are partly found within area of stress-corrosion fracture. Such a mixed-type fracture is shown in **Fig. 14**. From **Fig. 15** which shows a beam deflection vs time curve, it is obvious that the deflection increases discontinuously. The small periodic movements of the beam, however, occurred much more slowly rather than acoustically. From this it may be considered that the individual steps are associated with the discontinuous extensions of crack due to mechanical tearing of some areas on the cracking path. The bases of dimples on a mixed-type fracture are often containing inclusions, presumably manganese compounds $MnAl_6$. **Fig. 16** is an example

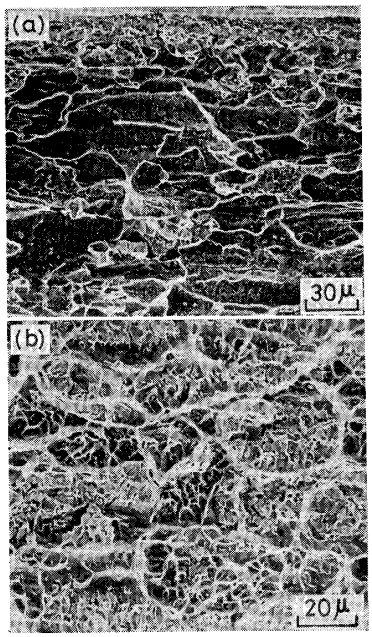

Fig. 13 Fracture surface of stress-corrosion cracked specimen heated 60 days at 100°C, showing typical integranular stress corrosion crack (a) and dimple pattern obtained in mechanical final fracture (b)

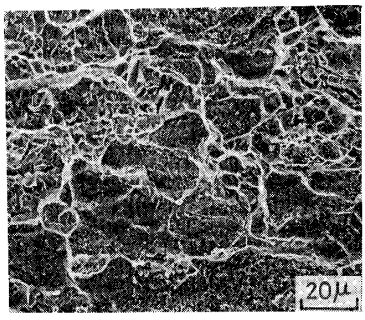

Fig. 14 Mixed-type fracture, fine dimples due to mechanical rupture found within area of intergranular stress-corrosion fracture.

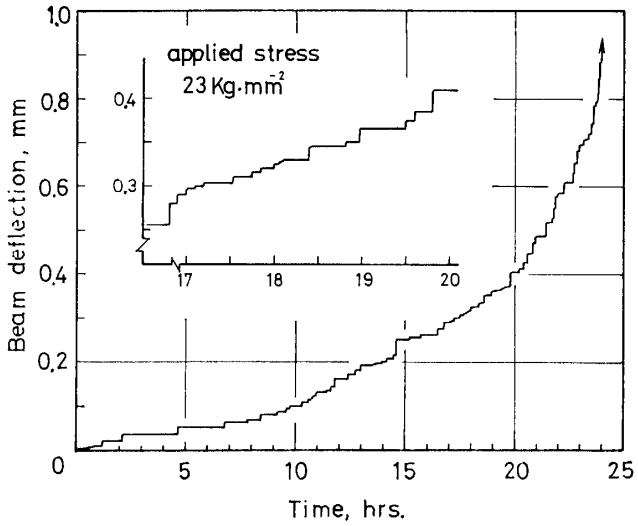

Fig. 15 Beam deflection vs time curve for the S.C.C. specimen heated 30 days at 100°C.

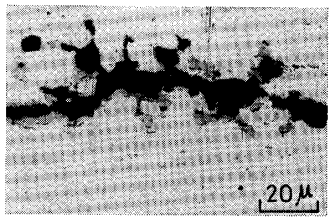

Fig. 16 Micro crack initiated at inclusions ($MnAl_6$) during tensile test on a specimen heated 60 days at 100°C.

of a micro crack initiated at a group of $MnAl_6$ during tensile test. These compounds seem to be brittle and to be readily ruptured mechanically. Furthermore, because the potential of $MnAl_6$ is pretty more noble than β phase[3], these existing on a cracking path may be ruptured by mechanical action rather than removed by dissolution.

When the precipitate at the grain boundaries is not present as a continuous film, on the corresponding fracture appearance the contribution of mechanical rupture becomes to be predominant. As shown in **Fig. 17**, corrosion tunnels are formed at grain boundaries as a result of dissolution at some points with the precipitate, while other

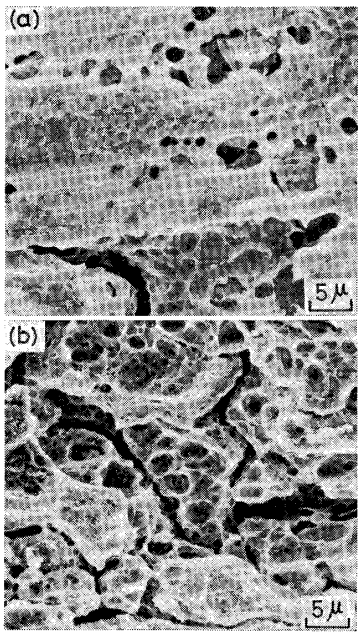

Fig. 17 Stress-corrosion fracture surfaces for 200°C 1 week heated specimen with lower sensitivity, showing corrosion tunnels (a) and the increased evidence of ductility (b).

points without the precipitate remain intact. When the local load sustained by these sound bridges[10] rises above a critical level, they rupture mechanically, fine dimples left on fracture surface as the evidence of ductile tear (Fig. 17–b).

The fractographic observations show that the stress-corrosion cracking occurs by a combination of mechanical and intergranular stress-corrosion fracture. Mechanical rupture plays a function to separate the higher-resistant areas to intergranular corrosion and may facilitate the propagation of stress-corrosion crack, while it does not appear to govern directly the propagation. The process of cracking may be essentially under the control of intergranular corrosion enhanced by a mechano-chemical effect.

Conclusion

The results may be summarized as follows.

1) Intergranular corrosion and stress-corrosion cracking are closely correlated with the precipitation of β phase and both occur extremely when this precipitate is quite continuous at grain boundaries.

2) The crack propagation rate can be expressed as an exponential function of the intergranular corrosion rate, which may be enhanced in proportion to the square of the applied stress.

3) The crack propagation is discontinuous and the contribution of mechanical rupture is found in the process of cracking.

4) Mechanical rupture, however, plays only a supplemental part. The stress-corrosion cracking may be essentially a manifestation of intergranular corrosion facilitated by a mechano-chemical effect.

Acknowledgement

The author would like to thank Prof. T. Takahashi of Tokyo Institute of Technology for steady consideration and advice. He is also deeply indebted to Dr. A. Kamio, Mr. Y. Kojima and the members of Takahashi laboratory for encouragement and advice during the course of this investigation.

References

1) E. C. W. Perryman and G. B. Broock: J. Inst. of Metals, **79**, Part 1, 19 (1951)
2) A. Eikum and G. Thomas: Acta Metallurgica, **12**, 537 (1964)
3) D. O. Sprowls and R. H. Brown: Proceedings of Conference on Foundamental Aspects of Stress Corrosion Cracking, Ohio State University, 469 (1967)
4) E. C. W. Perryman and S. E. Hadden: J. Inst. of Metals, **77**, 207 (1950)
5) E. H. Dix, Jr., W. A. Anderson and M. B. Shumaker: Corrosion, **15**, 2, 55t (1959)
6) H. L. Logan: The Stress Corrosion of Metals, Wiley, New York, 193 (1966)
7) R. B. Mears, R. H. Brown and E. H. Dix, Jr.: Symposium on Stress Corrosion Cracking of Metals, ASTM–AIME 329 (1944)
8) A. J. McEvily, Jr. and A. P. Bond: J. Electrochem. Soc., **112**, 2, 131 (1965)

9) N. A. Nielsen: Proceedings of Conference on Foundamental Aspects of Stress Corrosion Cracking, Ohio State University, 308 (1967)
10) W. J. Helfrich: Corrosion, **29**, 8, 316 (1973)